Supplementary Information

Introduction of a Multifunctional Percolated Framework into Na Metal for Highly Stable Sodium Metal Batteries

Sikandar Iqbal [a, b, c 1], Aadil Nabi Chishti [a, c 1], Moazzam Ali [a], Javed Rehman [d], Fakhr uz Zaman [e], Ting Luo [f], Muhammad Ali [a, c], Samia Aman [a, c], Hamid Hussain [a, c], Huiqin Huang [a, c], Shakeel Ahmad Khandy [a, c], Yinzhu Jiang [a, c *], Muhammad Yousaf [a*]

[a]ZJU-Hangzhou Global Scientific and Technological Innovation Center, Zhejiang University, Hangzhou, 310027, China
[b]Institute of Energy Materials Science (IEMS), University of Shanghai for Science and Technology, Shanghai 200093, China
[c]School of Materials Science and Engineering, Zhejiang University, Hangzhou, 310027, China
[d]State Key Laboratory of Metastable Materials Science and Technology, and School of Materials Science and Engineering, Yanshan University, Qinhuangdao 066004, China
[e]Institute for Advance Study Shenzhen University, Shenzhen 518060, China
[f]Department of Mechanical Engineering, Qilu University of Technology (Shandong Academy of Sciences), Jinan 250000, China

*Corresponding author‘s E-mail: muhammadyousaf@zju.edu.cn (M.Y.); yzjiang@zju.edu.cn (Y.Z.)

*Corresponding author‘s E-mail: muhammadyousaf@zju.edu.cn (M.Y.); yzjiang@zju.edu.cn (Y.Z.)

[1] These authors contributed equally to this work.

Contents

Fig. S6. Thickness of (a) bare Na, and (b) Na@NPC/Na_2Se electrode. Digital photographs of the c-e) bare Na, and f-h) Na@NPC/Na_2Se electrode.

Fig. S7. SEM of the bare Na.

Fig. S8. SEM of the Na@NPC/Na_2Se.

Fig. S9. XPS spectra of the N in the Na@NPC/Na_2Se.

Fig. S10. XPS spectra of the Na in the bare Na and Na@NPC/Na_2Se electrode.

Fig. S11. AFM of the bare Na electrode.

Fig. S12. EIS spectra of the bare Na and Na@NPC/Na_2Se electrode.

Fig.S13 CV of the Na@NPC@Na_2Se /Cu half battery.

Fig. S14. Electrochemical performance of the bare Na electrode in ether base electrolyte dissolved in diglyme.

Fig. S15. Electrochemical performance of the NPC modified Na electrode in ether base electrolyte dissolved in diglyme.

Fig. S16. Electrochemical performance of the Se modified Na electrode in ether base electrolyte dissolved in diglyme.

Fig. S17. Electrochemical performance of the modified Na electrode in carbonate electrolyte dissolved in a) PC: EMC, b) EC: PC: DEC.

Fig. S18. The rate capability of the bare Na electrode.

Fig. S19. EIS spectra of the bare Na electrode.

Fig. S20. Optimized structures of the Na, Na@NPC, Na@Se, and Na@NPC@Se.

Fig. 21. XPS of Na@NPC@Na_2Se electrode after plating. a) Individual XPS of a) Na-1s, b) Se-3d, c) and C1s respectively.

Fig. S22. a) Galvanostatic discharge and charge pleatues, b) CV of the Na@NPC/$Na_2Se||NVP$ and Na $||NVP$, respectively.

Materials and Methods

Synthesis of NPC

Analytical-grade zirconium chloride ($ZrCl_4$), terephthalic acid (H_2BDC), glacial acetic acid (HAc), and hydrofluoric acid solution (HF 40 %w/w) were obtained from Shanghai Chemical Reagents, China. All of the chemicals used in this experiment were analytical-grade and used without further purification. In a typical procedure for the synthesis of NPC, first, we dissolved H_2BDC (37.5 mg) and $ZrCl_4$ (52.5 mg) into DMF (50 mL) containing HAc (6 mL) and heated the solution at 120 ^oC for 16 h. After the reaction, the intermediate material was obtained by centrifugation, washing, and drying in the vacuum oven at 80 ^oC for 12 h. Subsequently, as prepared sample was heated at 800 ^oC under an Ar atmosphere for 4 h in the electric tube furnace. Thereafter, the black powder (100 mg) was dispersed in 40 mL of DI water containing 6 mL of HF solution and sonicated for 30 minutes. Finally, the NPC powder was obtained by centrifugation, washing, and drying.

Synthesis of NPC@Se composite

The NPC@Se composite was prepared by a solid-state selenization process. Specifically, NPC powder (100 mg) and Se powder (300 mg) with a mass ratio of 1:3 were placed in the porcelain boat and then heated the boat at 850 ^oC for 4 h with a ramping rate of 5 degrees/min in the tube furnace in Ar atmosphere. After the heat treatment, the tube furnace was naturally cooled to room temperature and got the product NPC@Se.

Fabrication of the Na@NPC/Na_2Se modified anode

The Na@NPC/Na_2Se foil was prepared by thermal and mechanical treatment in an Ar-filled glove box (O_2 and H_2O < 0.1 ppm). First, the Na metal was heated at 250 ^oC and then NPC@Se powder was added slowly into molten Na with continuous stirring for ~30 min until their uniform composite was attained. After cooling to room temperature, repeated rolling and folding operations (10 times) were performed on modified Na foil. The ratio of sodium metal to NPC@Na_2Se in the synthesis of the sodium metal negative electrode was chosen to be 7:1. After rest, the Na@NPC/Na_2Se foil was punched into 10 mm discs as electrodes for electrochemical testing

Fabrication of $Na_3V_2(PO_4)_3$ (NVP) cathode electrode

The NVP was purchased from Hubei Ennaiji Company and directly used as cathode materials. The cathode electrode was fabricated by coating slurry mixed with conductive carbon (Super P) and poly (vinylidene fluoride) (PVDF) binder at a weight ratio of 7:2:1 in 1-methyl-2-pyrrolidone (NMP) solvent. The slurry was coated on Al foil and then dried under vacuum at 65 ^{o}C overnight. The electrodes were then cut into disks and maintain the mass loading of each electrode was 3.0 mg cm^{-2}.

Electrochemical measurements

All batteries (2032-type coin cells) were assembled in Ar filled glove box using a Whatman GF/D glass fiber as a separator with a 200 μL standard amount of the electrolyte for all kinds of cells. The 1.0 M of $NaClO_4$ in PC: EC (1:1 in volume ratio) was used as a carbonate-based electrolyte, while $NaPF_6$ dissolved in diglyme was used as the ether-based electrolyte in symmetric cells. Notably, only ether base-based electrolyte ($NaPF_6$ dissolved in diglyme) was used in full cells. The electrochemical performance of each cell was measured using Neware testing instrument (BTS-610). Electrochemical impedance spectroscopy (EIS) was conducted through a sine wave with an amplitude of 5 mV over a frequency range from 100 kHz to 10 MHz on an electrochemical workstation (CHI 660D, Chenhua Instrument Company, Shanghai, China).

Materials Characterization

The crystal structures were obtained by applying X-ray diffraction (XRD, Bruker) with Cu Kα radiation at a scan rate of 10° min^{-1}. The microstructures and surface morphologies were investigated through transmission electron microscopy (TEM) and high-resolution TEM, and scanning emission microscopy (SEM, JEOL, JSM 6360LA). The surface chemical information of modified Na before and after cycling was verified by X-ray photoelectron spectroscopy (XPS, Thermo Fisher ESCALAB 250Xi). The surface roughness and young modulus were measured using atomic force microscopy (AFM, MFP-3D-Stand Alone, Asylum Research)

Theoretical calculations

The first principle calculations are performed by Vienna Ab initio Simulation Package (VASP) with the projector augmented wave (PAW) method. The exchange-functional is treated using the Perdew-Burke-Ernzerhof (PBE) functional. The calculations were performed in a spin-polarized manner. The cut-off energy of the plane-wave basis is set at 550 eV. For the optimization of both geometry and lattice size, the Brillouin zone integration is performed with 5*5*2 Monkhorts-Pack k point sampling. The self-consistent calculations apply a convergence energy threshold of 10^{-5}

eV. The equilibrium geometries and lattice constants are optimized with maximum stress on each atom within 0.02 eV/Å.

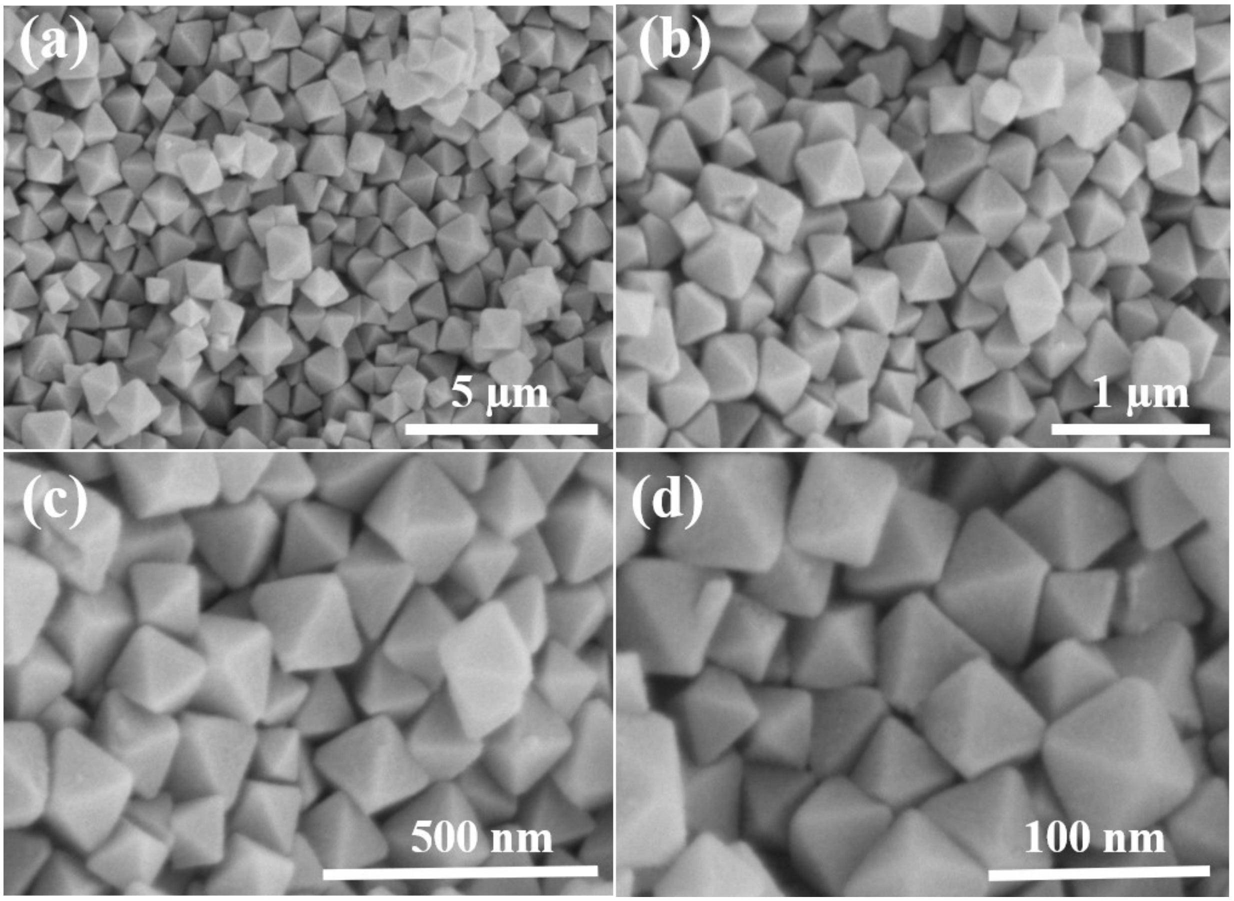

Fig. S1. SEM of UIO-66 MOF precursor.

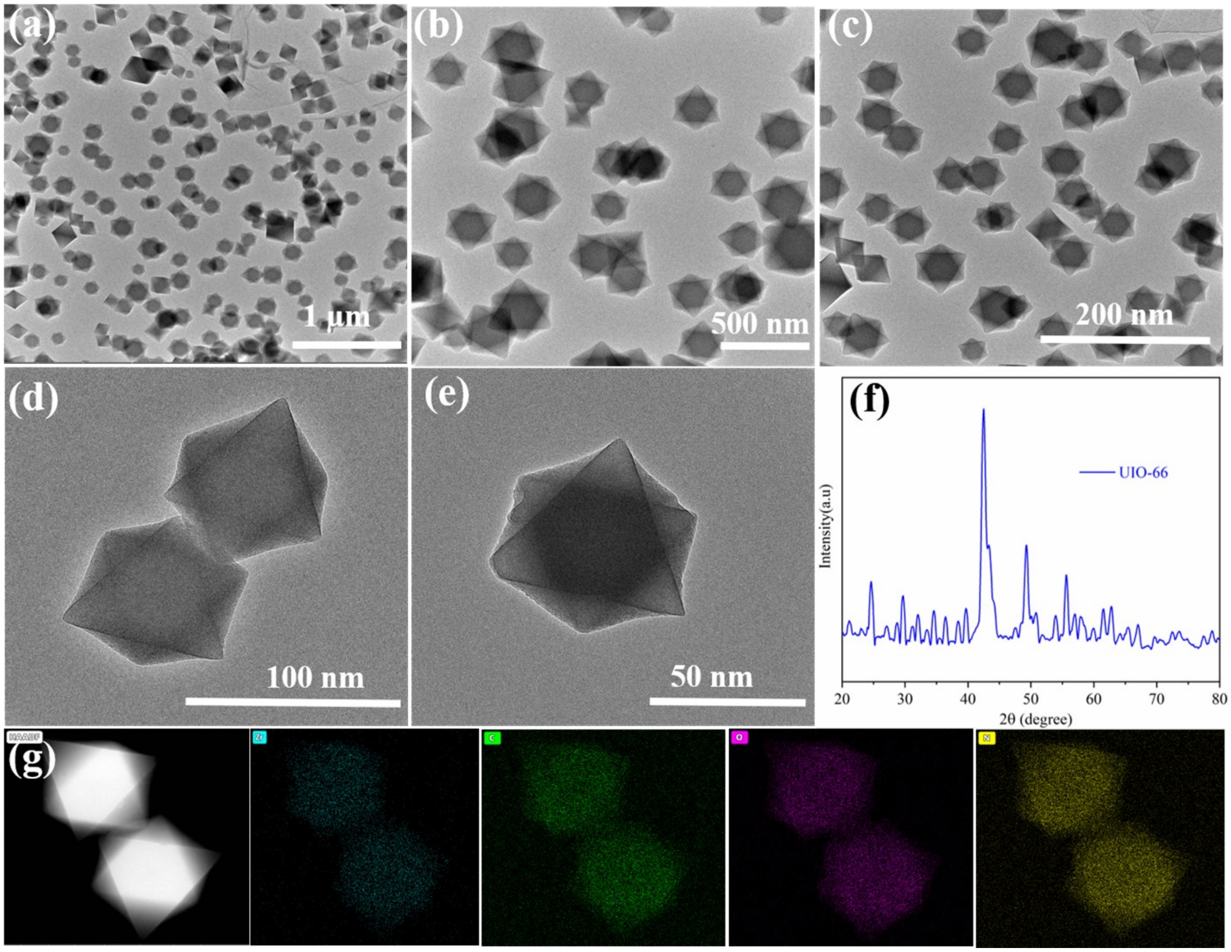

Fig. S2. a-c) TEM d, e) HRTEM, f) XRD, and g) elemental mapping of UIO-66 MOF precursor.

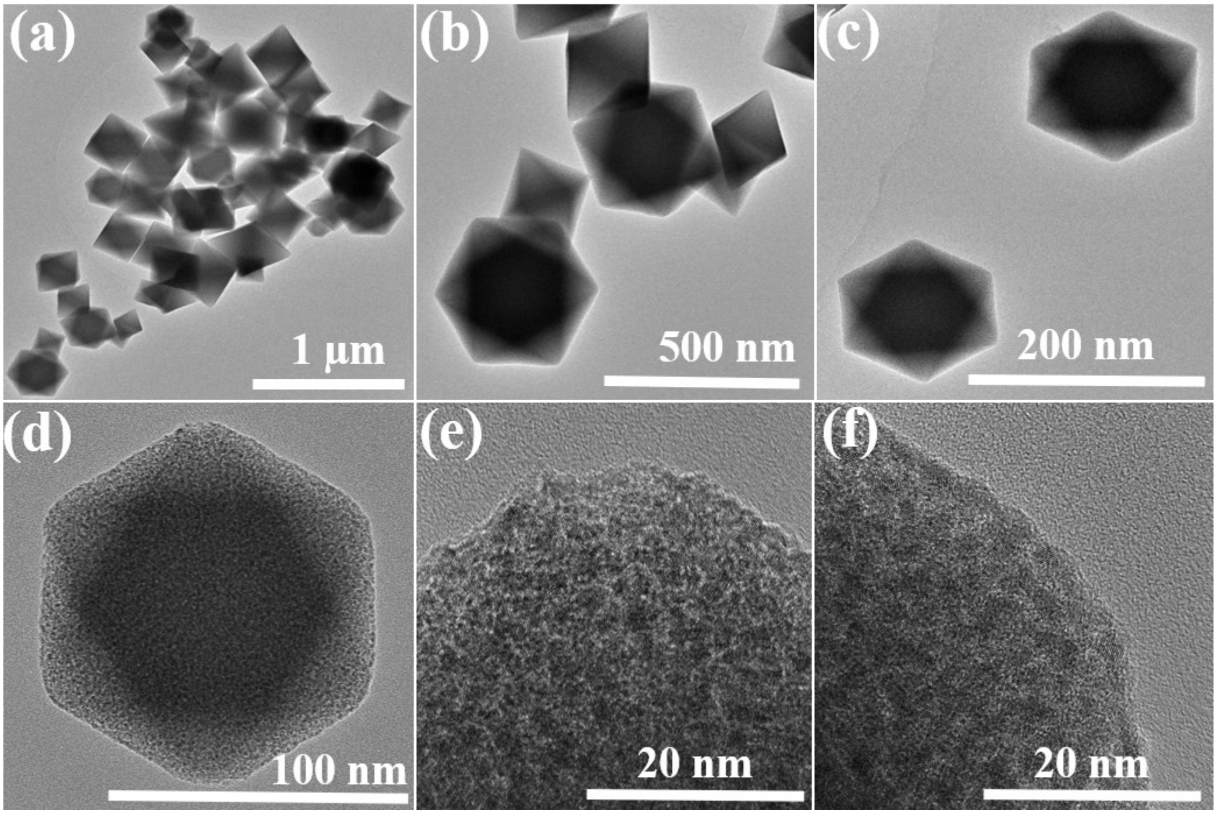

Fig. S3. a-c) TEM d-f) HRTEM of the ZrO_2.

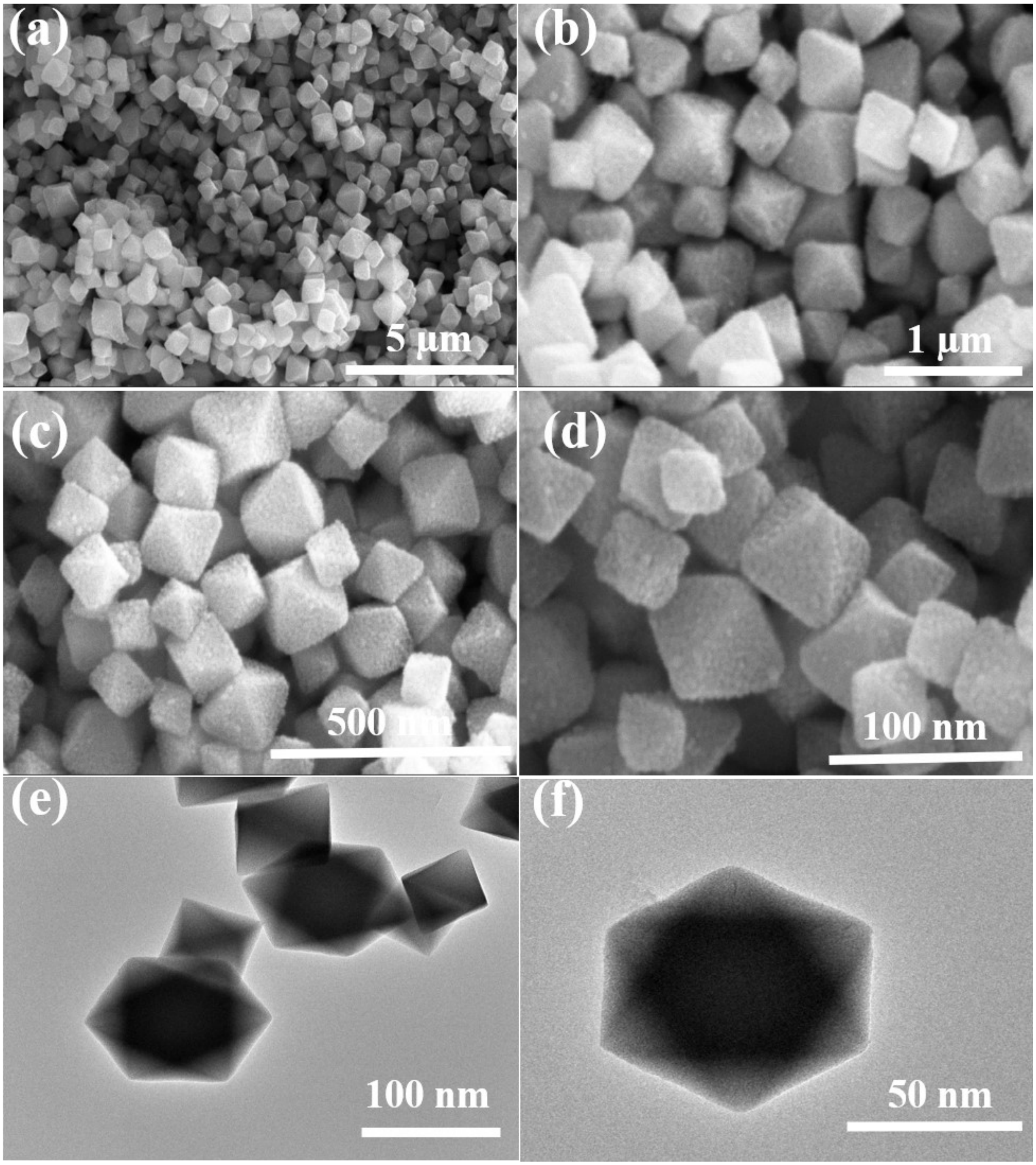

Fig. S4. a-d) SEM, and e-f) TEM of the porous carbon (NPC).

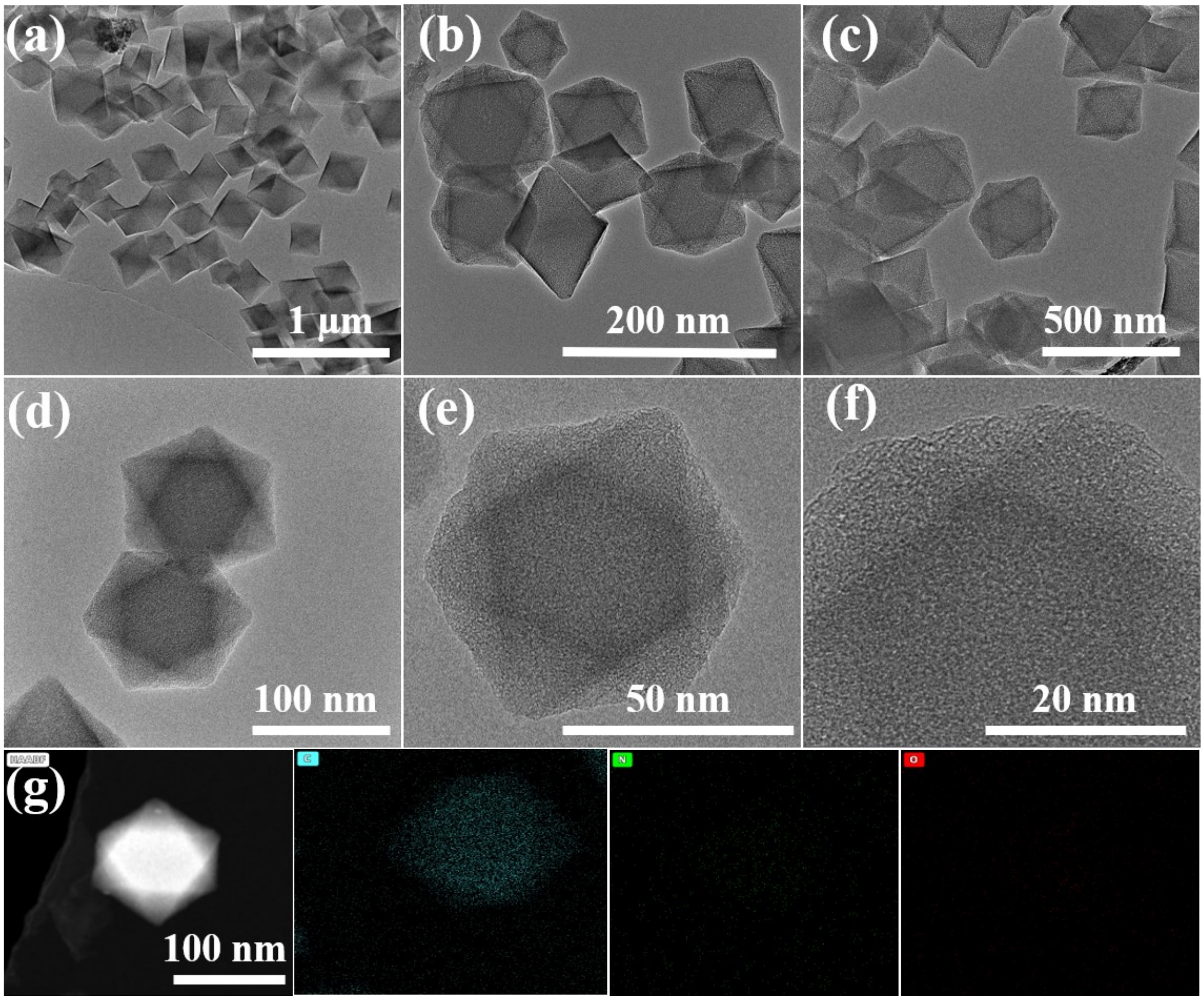

Fig. S5. a-d) TEM e, f) HRTEM, and g) elemental mapping of NPC.

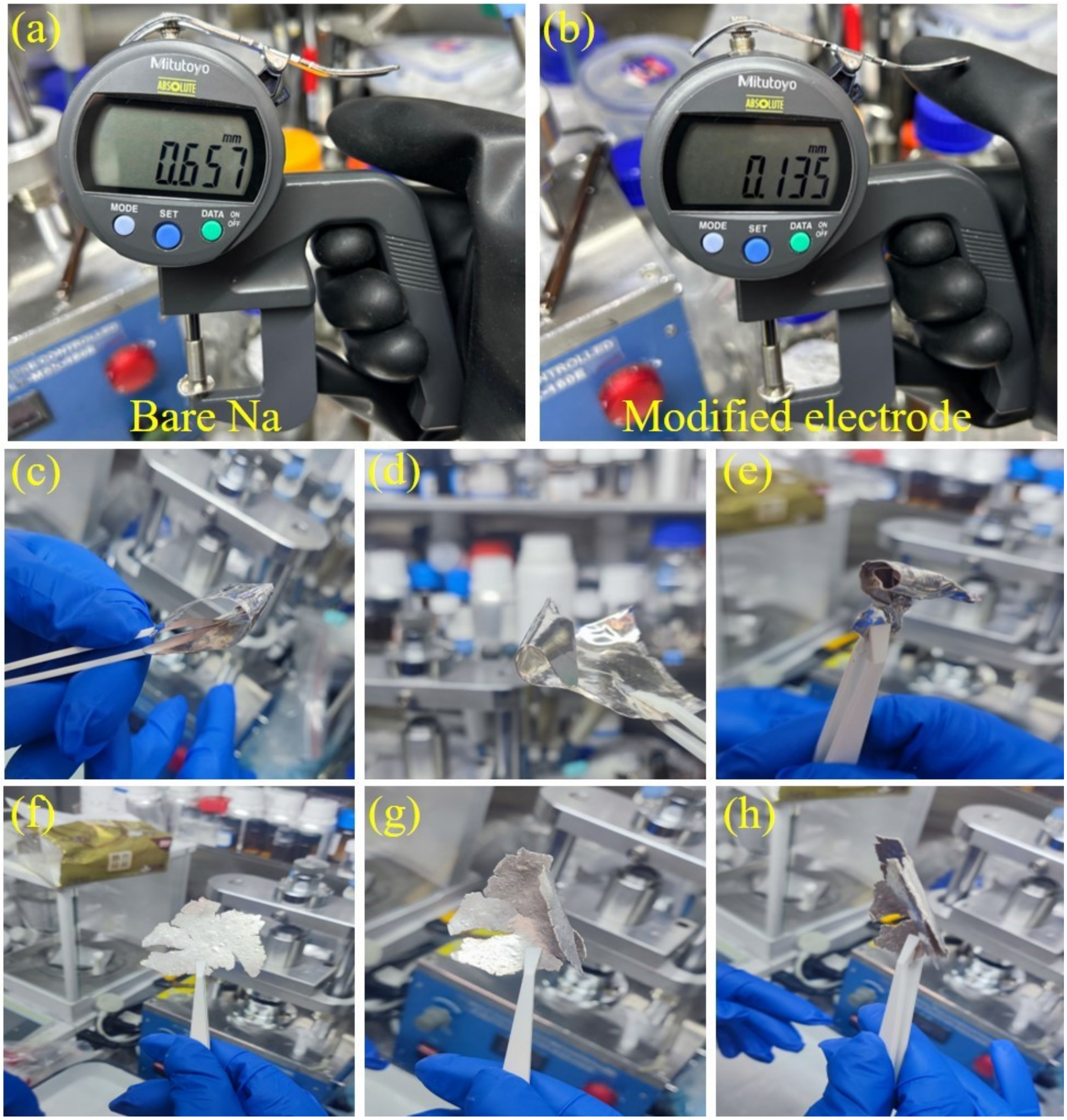

Fig. S6. Thickness of (a) bare Na, and (b) Na@NPC/Na_2Se electrode. Digital photographs of the c-e) bare Na, and f-h) Na@NPC/Na_2Se electrode.

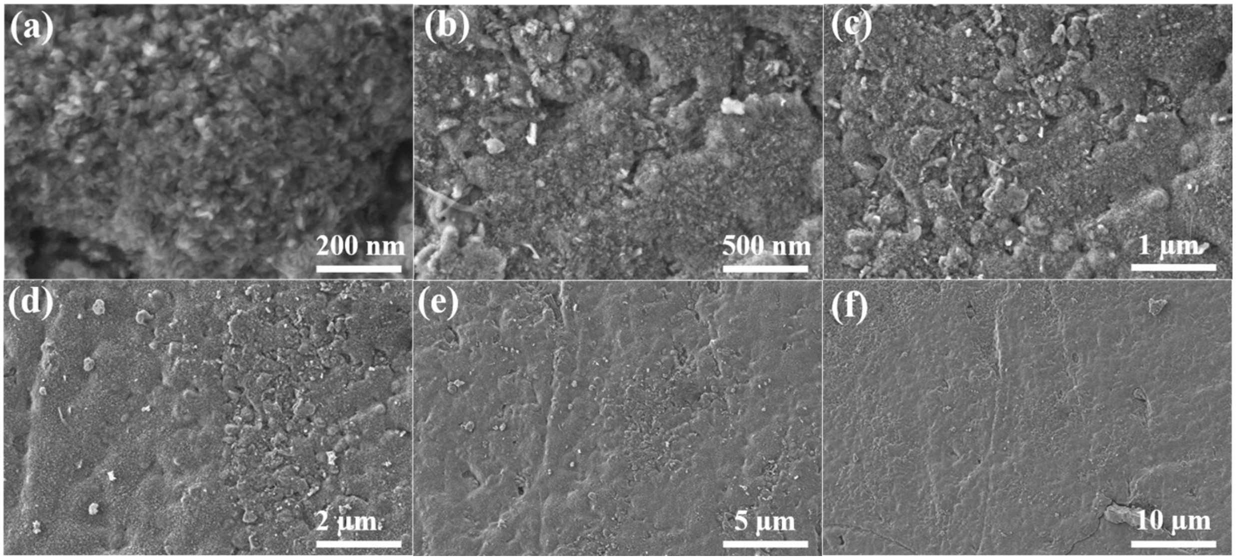

Fig. S7. SEM of the bare Na.

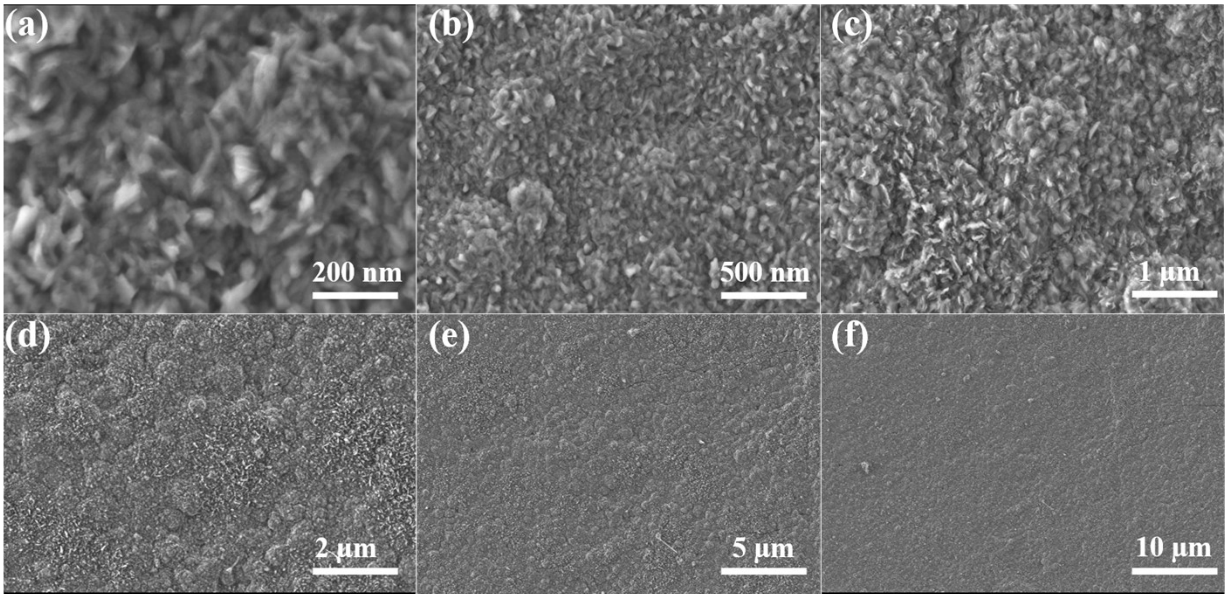

Fig. S8. SEM of the Na@NPC/Na_2Se.

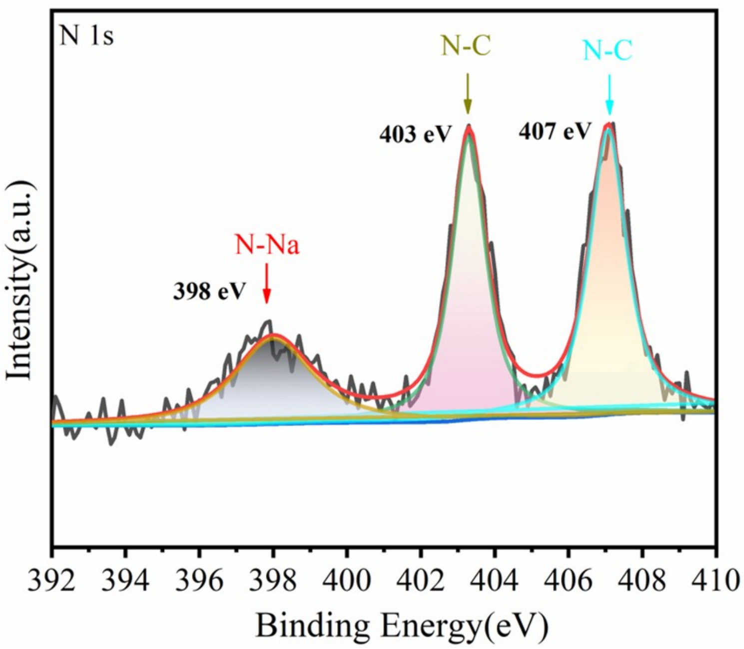

Fig. S9. XPS spectra of the N in the Na@NPC/Na_2Se.

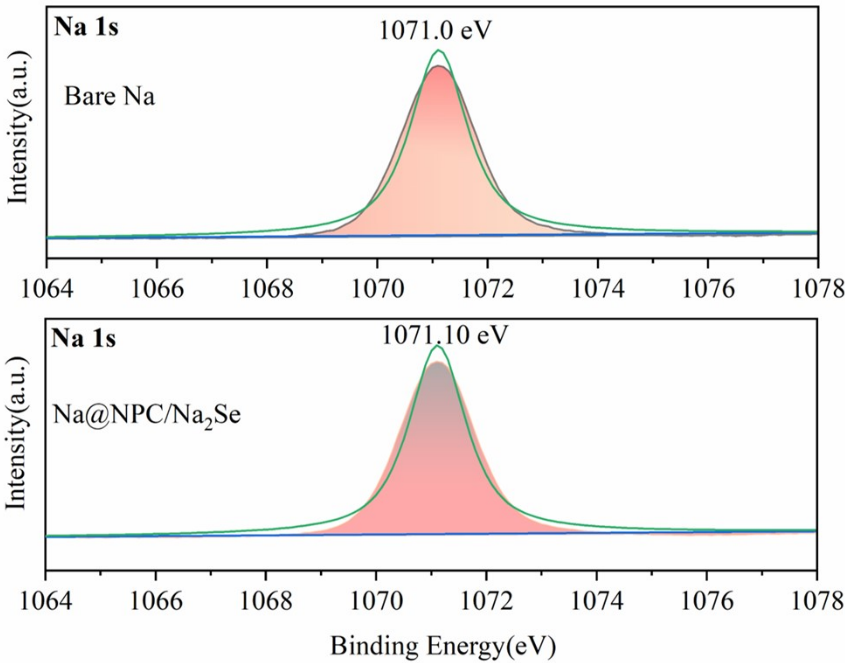

Fig. S10. XPS spectra of the Na in the bare Na and Na@NPC/Na_2Se electrode.

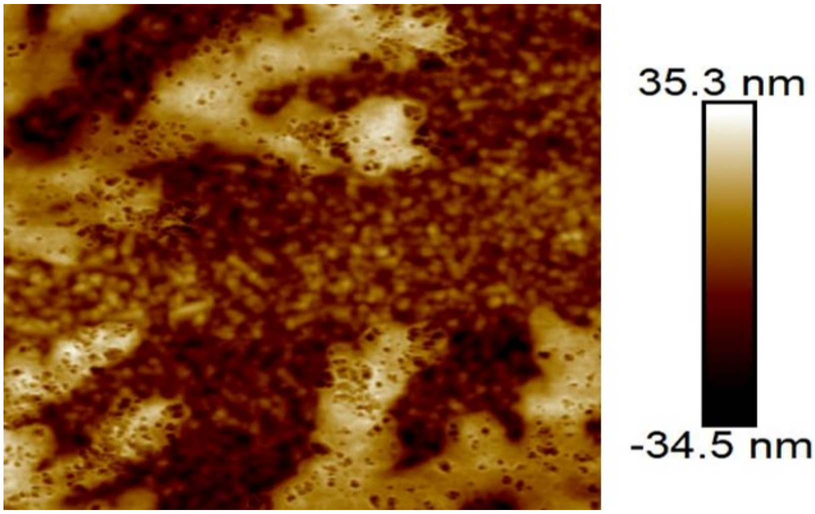

Fig. S11. AFM of the bare Na electrode.

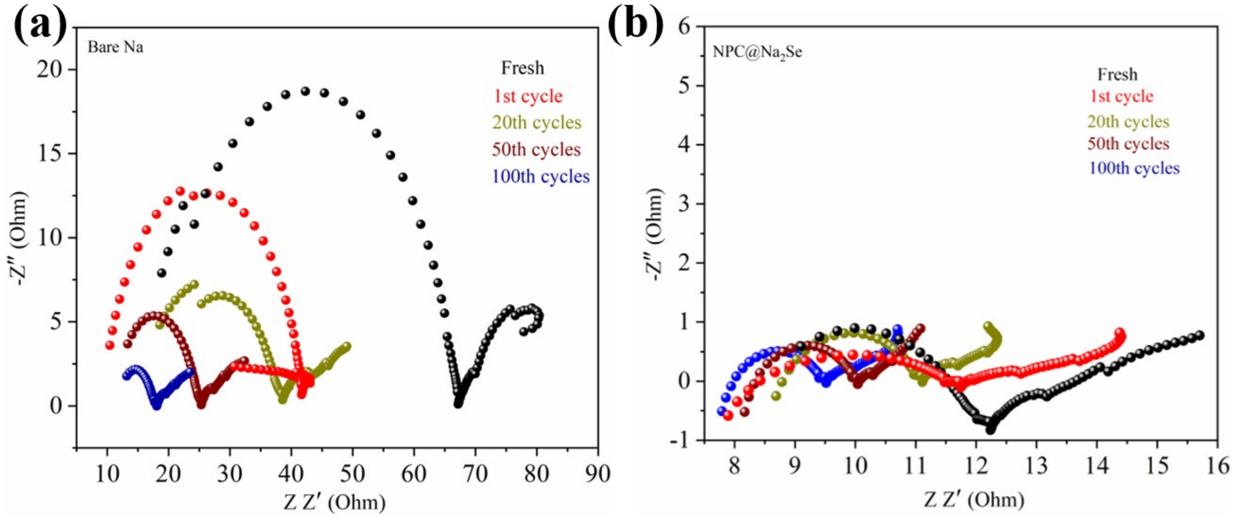

Fig. S12. EIS spectra of the bare Na and Na@NPC/Na$_2$Se electrode in ether base electrolyte.

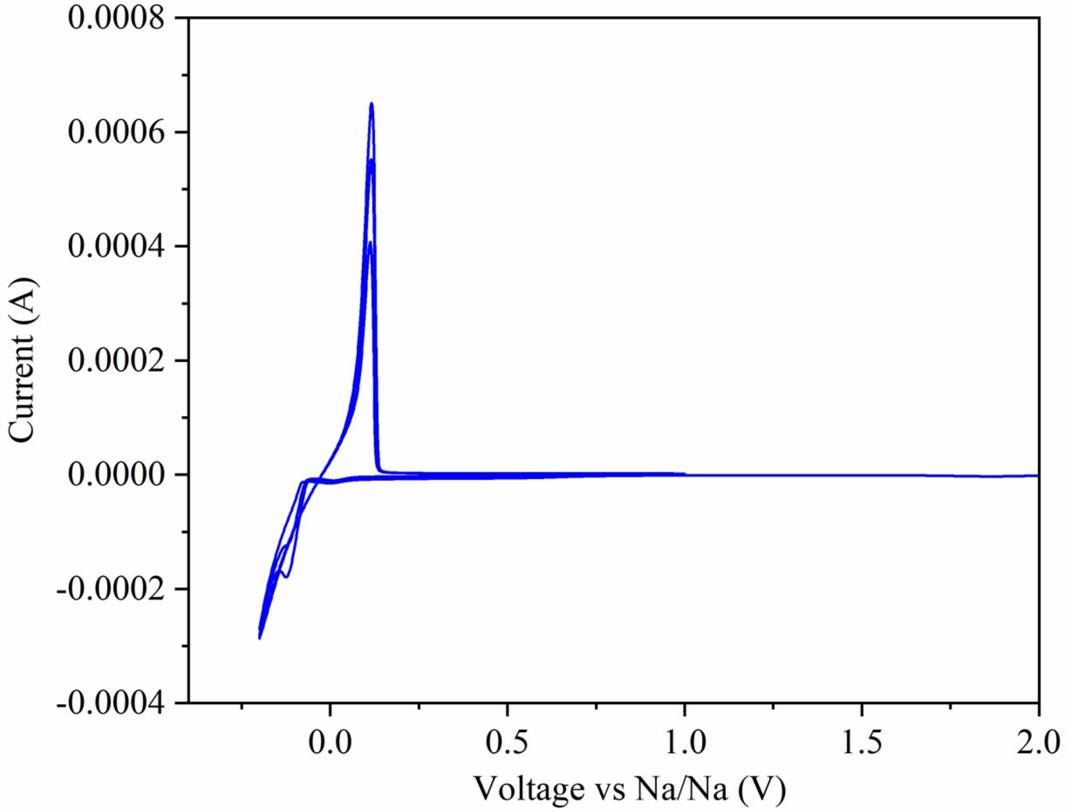

Fig.S13 CV of the Na@NPC@Na_2Se /Cu half battery.

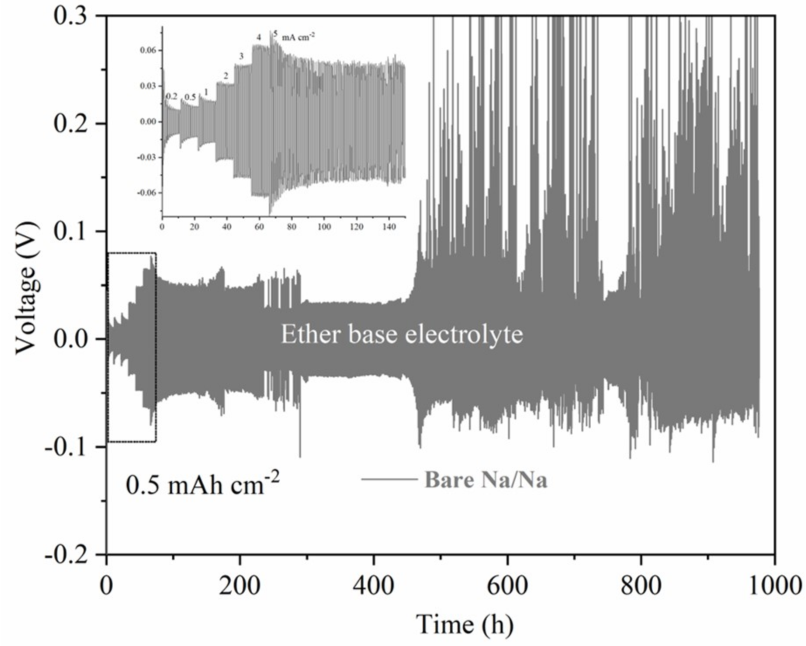

Fig.S14. Electrochemical performance of the bare Na electrode in ether base electrolyte dissolved in diglyme.

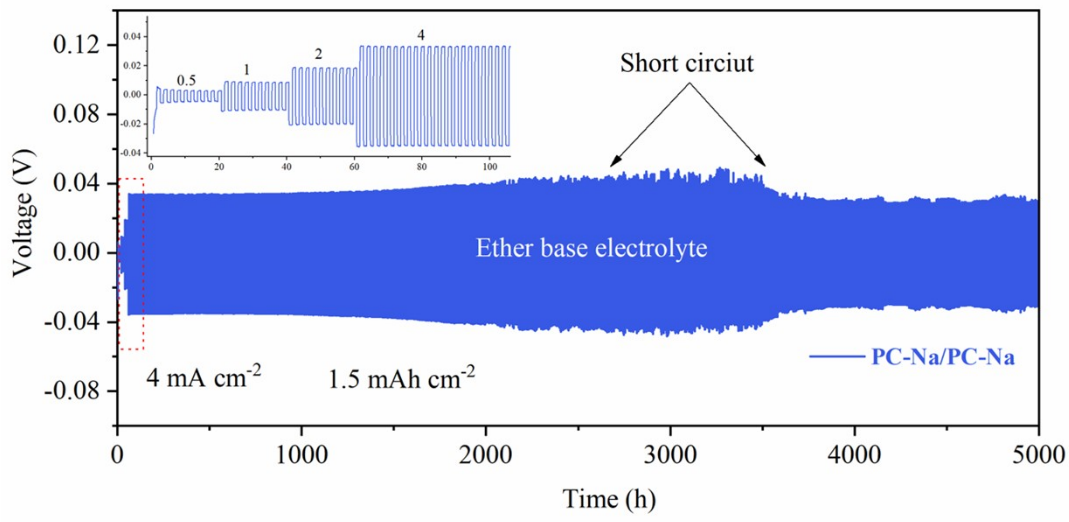

Fig. S15. Electrochemical performance of the NPC modified Na electrode in ether base electrolyte dissolved in diglyme.

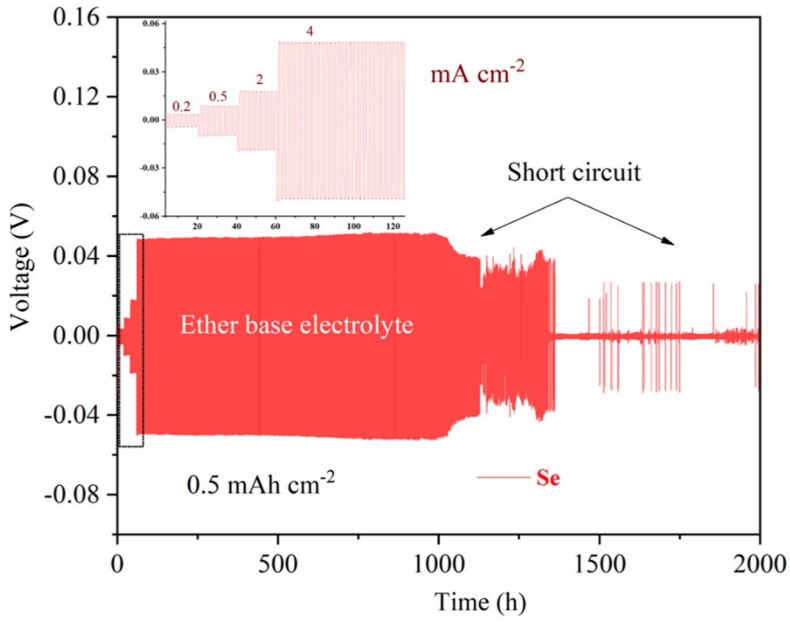

Fig. S16. Electrochemical performance of the Se-modified Na electrode in ether base electrolyte dissolved in diglyme.

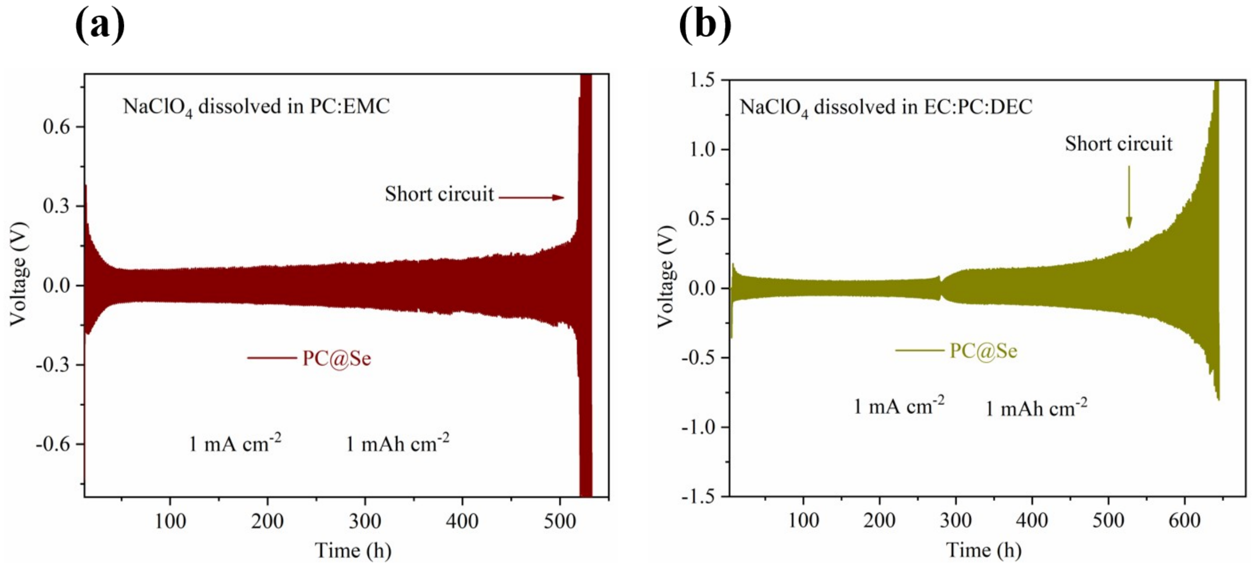

Fig.S17. Electrochemical performance of the modified Na electrode in carbonate electrolyte dissolved in a) PC: EMC, b) EC: PC: DEC.

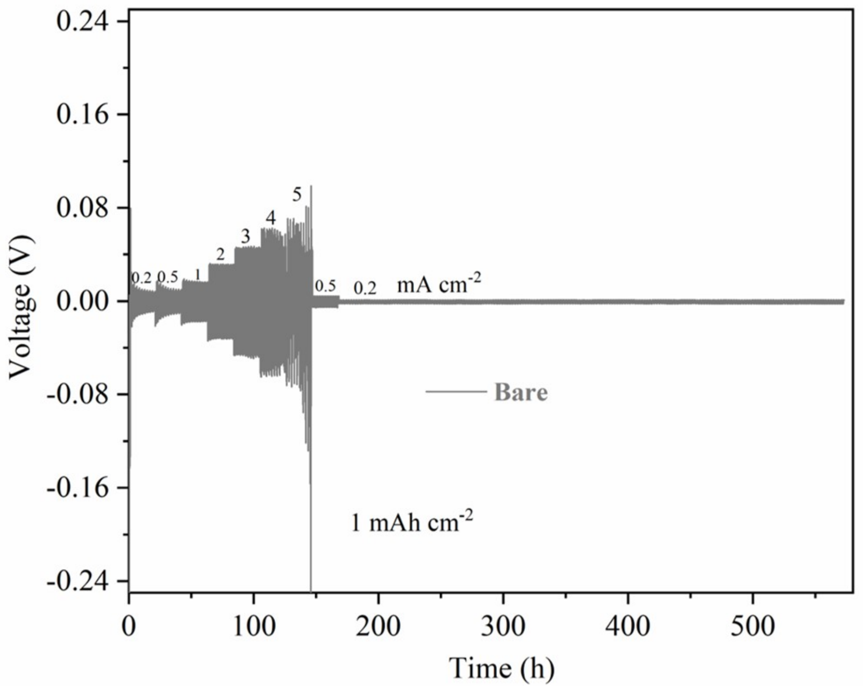

Fig. S18. The rate capability of the bare Na electrode.

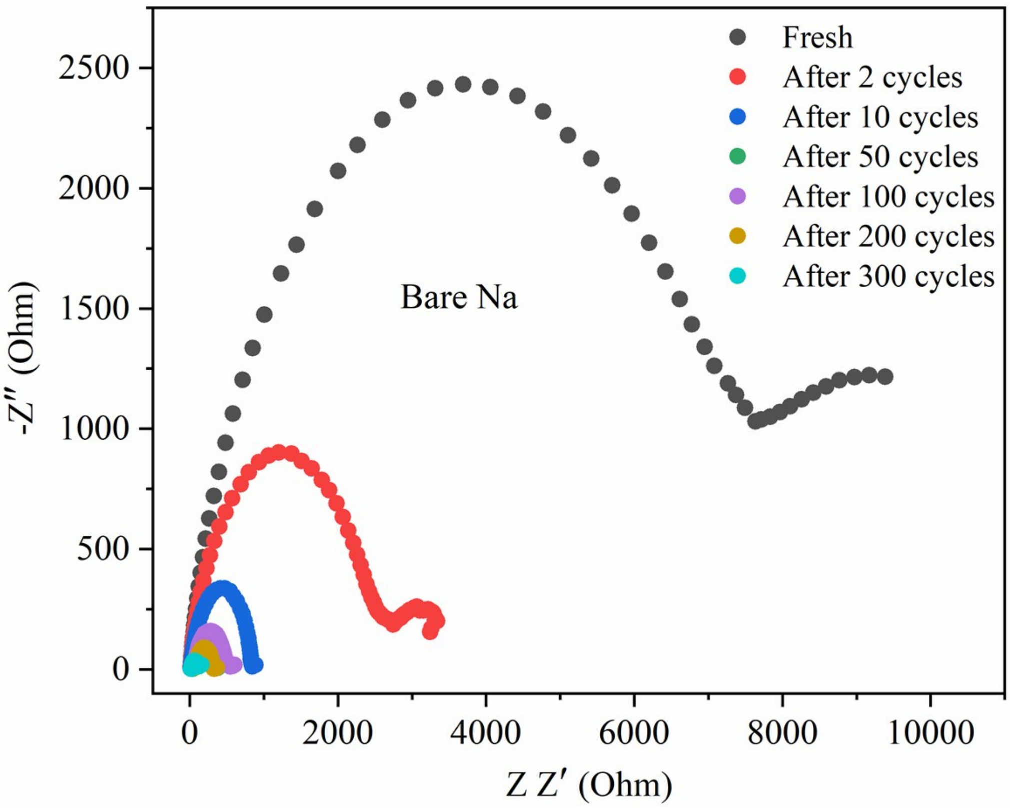

Fig. S19. EIS spectra of the bare Na electrode.

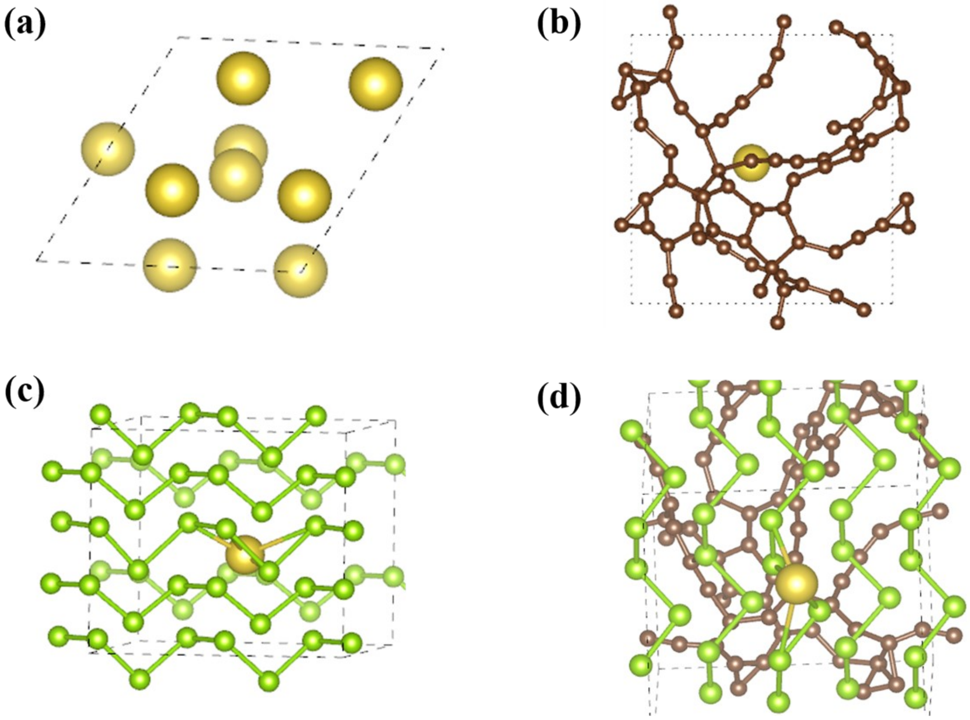

Fig. S20. Optimized structures of the Na, Na@NPC, Na@Se, and Na@NPC@Se.

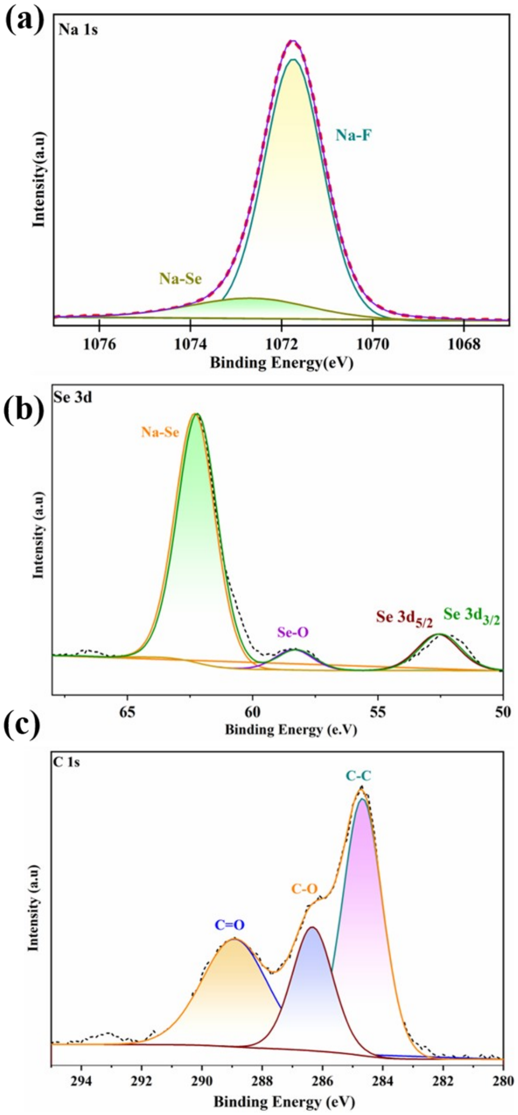

Fig. 21. XPS of Na@NPC@Na_2Se electrode after plating. a) Individual XPS of a) Na-1s, b) Se-3d, c) and C1s respectively.

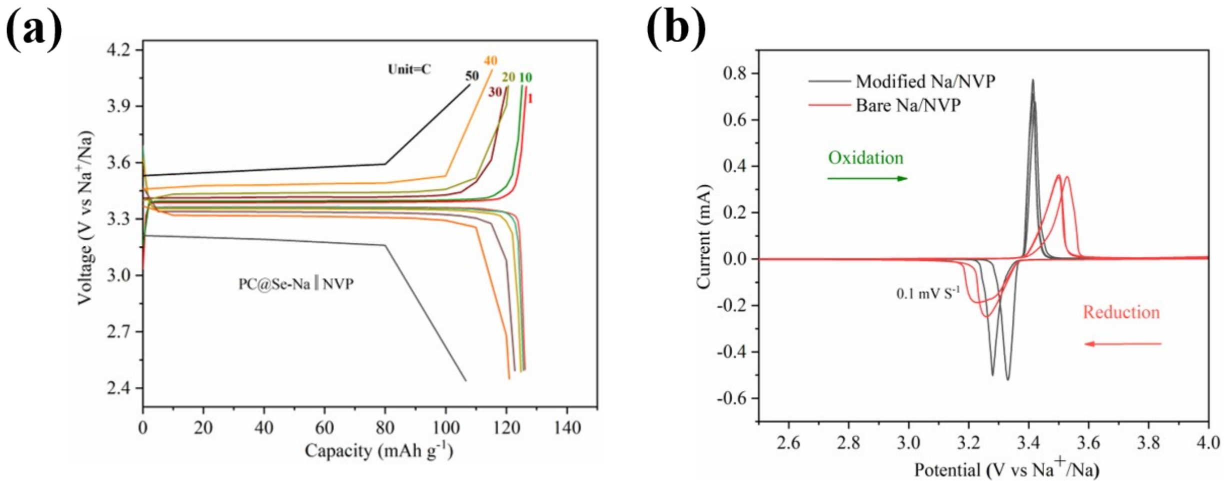

Fig. S22. a) Galvanostatic discharge and charge pleatues, b) CV of the Na@NPC@Na$_2$Se||NVP and Na ||NVP, respectively.